Chem Biol Drug Des 2006; **67:** 215–229

doi: 10.1111/j.1747-0285.2006.00362.x

Research Article

Molecular Mechanism of the Constitutive Activation of the L250Q Human Melanocortin-4 Receptor Polymorphism‡

Bettina Proneth[1†], Zhimin Xiang[1†], Irina D. Pogozheva[2], Sally A. Litherland[3], Oleg S. Gorbatyuk[1], Amanda M. Shaw[4], William J. Millard[4], Henry I. Mosberg[2] and Carrie Haskell-Luevano[1]*

[1]*Department of Medicinal Chemistry, University of Florida, PO Box 100485, Gainesville, FL 32610-0485, USA*
[2]*Department of Medicinal Chemistry, University of Michigan, Ann Arbor, MI 48109, USA*
[3]*Department of Pathology, Immunology and Laboratory Medicine, University of Florida, Gainesville, FL 32610, USA*
[4]*Department of Pharmacodynamics, University of Florida, Gainesville, FL 32610, USA*
**Corresponding author: Carrie Haskell-Luevano, carrie@cop.ufl.edu*

The Melanocortin-4 Receptor is a G-protein coupled receptor that has been physiologically linked to participate in the regulation of energy homeostasis. The Melanocortin-4 Receptor is stimulated by endogenous melanocortin agonists derived from the pro-opiomelanocortin gene transcript and antagonized by the endogenous antagonist agouti-related protein. Central administration of melanocortin agonists has been demonstrated to decrease food intake and conversely, treatment with antagonists resulted in increased food intake. Deletion of the Melanocortin-4 Receptor gene from the mouse genome results in an obese and hyperphagic phenotype. Polymorphisms of the human Melanocortin-4-Receptor have been found in severely obese individuals, suggesting that Melanocortin-4 Receptor malfunction might be involved in human obesity and obesity-associated diabetes. Herein, we have performed experiments to understand the molecular mechanisms associated with the L250Q human Melanocortin-4-Receptor polymorphism discovered in an extremely obese woman. This L250Q human Melanocortin-4-Receptor has been pharmacologically characterized to result in a constitutively active receptor. The fact that a constitutively active human Melanocortin-4-Receptor mutation was found in an obese person is a physiologic contradiction, as chronic activation of the human Melanocortin-4-Receptor and subsequently high cyclic adenosine monophosphate levels should theoretically result in a normal or lean phenotype. In this study, we demonstrated that agouti-related protein acts as an inverse agonist at this constitutively active receptor, and we propose a mechanism by which agouti-related protein might contribute to the obese phenotype in the L250Q patient. In addition, using receptor mutagenesis, pharmacology, and computer modeling approaches, we investigated the molecular mechanism by which modification of the L250 residue results in constitutive activation of the human Melanocortin-4-Receptor.

Key words: agouti-related protein, constitutive activation, G-protein coupled receptor, melanotropin, obesity, AGRP, POMC

Received 18 January 2006, revised and accepted for publication 2 February 2006

The melanocortin system consists of five melanocortin receptors (MCRs) that are expressed differentially throughout the body and belong to the superfamily of G-protein coupled receptors (GPCRs) that stimulate the cyclic adenosine monophosphate (cAMP) signal transduction pathway (1–7). The melanocortin pathway includes endogenous agonists and the only two known endogenous antagonists of GPCRs, agouti and agouti-related protein (AGRP) (8,9). The melanotropin peptides, α-, β- and γ-melanocyte-stimulating hormone (MSH) and adrenocorticotropin hormone (ACTH), are the endogenous agonists of the MCRs that are derived by posttranslational processing of the precursor hormone pro-opiomelanocortin (POMC) (10,11). Physiologically, the melanocortin system has been identified to participate in the regulation of feeding behavior, obesity, and energy homeostasis in rodents as well as in humans (12–18). It has been demonstrated that targeted disruption of the Melanocortin-4 Receptor (MC4R) gene in mice results in hyperphagia, obesity, increased linear growth, and hyperinsulinemia (16). Additionally, pharmacologic studies of intracerebroventricular (ICV) injection of the synthetic melanocortin agonist MTII (19) inhibits feeding in mice, and this effect can be blocked by co-administration of the MC3R and MC4R antagonist SHU9119 (14,20). The endogenous MC3R and MC4R antagonist AGRP (8,21) when administered centrally, produces a sustained increase in food intake observed for days (22,23). Ectopic expression of the AGRP protein in transgenic mice results in hyperphagia and obesity (8,24). *In vitro* pharmacologic studies have demonstrated that AGRP is a competitive antagonist of α-MSH at the centrally expressing MC3R and MC4R (8), and also

†These authors contributed equally to this study.
‡This study is dedicated to Mrs Rozella May Haskell (lived between September 10, 1922 and May 6, 2005) who passed away due to complications of Type 2 Diabetes.

possesses inverse agonist activity at the MC4R (25–27). The inverse agonist activity of AGRP at the MC4R implicates an alternative physiologic mechanism of AGRP function in addition to simple competitive antagonism of α-MSH at MCRs.

In humans, more than 50 different single nucleotide polymorphisms (SNPs) of the MC4R gene have been discovered (17,18,28–47). One of these human MC4R polymorphisms, L250Q (GPCR residue i.d. = 6.40), is putatively located at the intracellular end of the transmembrane 6 (TM6) domain. The L250Q human Melanocortin-4-Receptor (hMC4R) was identified in an extremely obese French female patient and when characterized pharmacologically *in vitro*, resulted in the discovery of the first constitutively active hMC4R (17). Constitutive activation of the L250Q hMC4R resulted in elevated basal cAMP levels of the receptor in the absence of agonist stimulation (17). The fact that a constitutively active hMC4R mutation was found in an obese person is a paradox, because chronic activation of the hMC4R and subsequently high cAMP levels should theoretically result in a normal or lean phenotype. Thus, the molecular mechanism by which this L250Q hMC4R polymorphism is involved in human obesity is not yet understood at a molecular level and initiated the study reported herein.

Materials and Methods

Materials

Peptides used in this study were purchased from commercial sources, α-MSH, 4-norleucine-7-D-phenylalanine (NDP)-MSH, MTII, ACTH(1–24), β-MSH, γ_2-MSH (Bachem, Terrance, CA, USA), and human Agouti-related Protein [hAGRP(87–132); Peptides International, Louisville, KY, USA]. The melanocortin tetrapeptide JRH887–9 (Ac-His-D-Phe-Arg-Trp-NH_2) was synthesized in our laboratory as previously reported (48).

hMC4R in vitro receptor mutagenesis

The human wild-type (WT) N-terminal Flag-tagged hMC4R cDNA was generously provided by Dr Robert Mackenzie (30), and was subcloned into the pBluescript plasmid (Stratagene, La Jolla, CA, USA) for subsequent mutagenesis. *In vitro* hMC4R mutagenesis was performed as described previously (49). Amino acid modifications of the hMC4R were introduced by applying a polymerase chain reaction (PCR) strategy using pfu turbo polymerase (Stratagene) and a complementary set of primers containing the nucleotide mutation(s) resulting in the desired residue change. After completion of the PCR (95 °C for 30 s, 12 cycles of 95 °C for 30 s, 55 °C for 1 min, 68 °C for 9 min) the product was purified (Qiaquick PCR Purification Kit, Qiagen, Valencia, CA, USA) and eluted in water. Subsequently, the sample was cut with *Dpn*I (Invitrogen, Carlsbad, CA, USA) to linearize the WT template DNA leaving only nicked circularized mutant DNA. The mutant hMC4R DNA was then transformed into competent DH5α *Escherichia coli* cells. Single colonies were selected and the presence of the desired mutant was verified by DNA sequencing. The DNA containing the mutant was then excised and subcloned into the *Hin*dIII/*Xba*I restriction sites of the $pCDNA_3$ expression vector (Invitrogen). Complete Flag-hMC4R sequences were confirmed free of PCR nucleotide base errors by DNA sequencing (University of Florida sequencing core facilities).

Generation of stable cell lines

Human embryonic kidney-293 (HEK-293) cells were maintained as described previously (49) in Dulbecco's Modified Eagle's medium (DMEM) with 10% fetal calf serum and seeded 1 day prior to transfection at 1×10^6 cells/100-mm dish. Wild-type and mutant DNA in the $pCDNA_3$ expression vector (20 μg) were transfected using the calcium phosphate method (50). Stable receptor populations were generated using G418 selection (0.7–1 mg/mL) for subsequent bioassay analysis.

cAMP-based functional bioassay

Human embryonic kidney-293 cells stably expressing WT and mutant receptors were transfected with 4 μg of cAMP response element (CRE)/β-galactosidase reporter gene as previously described (49,51). Briefly, 5000–15 000 post-transfection cells were plated into collagen-treated 96-well plates and incubated overnight. Forty-eight hours post-transfection, the cells were stimulated with 100 μL of peptide (10^{-6} to 10^{-12} M) for α-MSH, NDP-MSH, and ACTH(1–24) and 100 μL of peptide (10^{-5} to 10^{-11} M) for γ_2-MSH, β-MSH, and JRH887–9 or forskolin (10^{-4} M) control in assay medium [DMEM containing 0.1 mg/mL bovine serum albumin (BSA) and 0.1 mM isobutylmethylxanthine] for 6 h. The assay media was aspirated and 50 μL of lysis buffer (250 mM Tris–HCl, pH 8.0, and 0.1% Triton-X-100) was added. The plates were stored at −80 °C overnight. The plates containing the cell lysates were thawed the following day. Aliquots of 10 μL were taken from each well and transferred to another 96-well plate for relative protein determination. To the cell lysate plates, 40 μL of phosphate-buffered saline (PBS) with 0.5% BSA was added to each well. Subsequently, 150 μL of substrate buffer [60 mM sodium phosphate, 1 mM $MgCl_2$, 10 mM KCl, 5 mM β-mercaptoethanol, 2 mg/mL of *o*-nitrophenyl-β-D-galactopyranoside (ONPG)] was added to each well and the plates were incubated at 37 °C. The sample absorbance, OD_{405}, was measured using a 96-well plate reader (Molecular Devices, Sunnyvale, CA, USA). The relative protein was determined by adding 200 μL 1:5 dilution Bio-Rad (Hercules, CA, USA) G250 protein dye:water to the 10 μL cell lysate sample taken previously, and the OD_{595} was measured on a 96-well plate reader (Molecular Devices). Data points were normalized both to the relative protein content and non-receptor-dependent forskolin values. Assays were performed using duplicate data points and repeated in at least three independent experiments. Data analysis, EC_{50}, pA_2 estimates, and their associated standard errors of the mean, were determined by fitting the data to a non-linear least-squares analysis using the PRISM program (v4.0, GraphPad Inc., San Diego, CA, USA). The antagonistic and inverse agonist properties of hAGRP(87–132) were determined by the ability of this ligand to competitively displace the MTII agonist in a dose-dependent manner. The pA_2 values were generated using the Schild analysis method (52). Statistical analysis was performed using a Student's *t*-test.

Transient transfection bioassay

Human embryonic kidney-293 cells were maintained in DMEM with 10% fetal calf serum and seeded 1 day prior to transfection at 2×10^6 cells/100-mm dish. Mutant and WT plasmid DNAs were transfected in a single experiment at different concentrations, as shown in Table 1, using the calcium phosphate method (50). Cells were incubated overnight at 35 °C and 3% CO_2, and the colorimetric reporter gene bioassays were performed as described above, with the exception that dose–response curves of compounds were omitted, only the basal and forskolin values were measured (49,53).

Table 1: Concentration of DNA used in the transient transfection assay

	Concentration plotted (ng)					
DNA transfected	0	5	25	50	75	100
Mutant/WT (ng)	0	5	25	50	75	100
$pCDNA_3$ plasmid (ng)	100	95	75	50	25	0
CRE/β-gal (μg)	4	4	4	4	4	4

WT, wild type; CRE, cyclic adenosine monophosphate response element.

Competitive displacement-binding assays

NDP-MSH and hAGRP(87–132) iodination

^{125}I-NDP-MSH and ^{125}I-AGRP(87–132) were prepared using a modified chloramine-T method as previously described (54). Using 50 mM sodium phosphate buffer (pH 7.4) as the reaction buffer, ^{125}I-Na (0.5 mCi; Amersham Life Sciences, Inc., Piscataway, NJ, USA) was added to 20 μg of NDP-MSH (Bachem) or 20 μg AGRP(87–132) (Peptides International) in 5 μL buffer. To initiate the reaction, 10 μL of a 2.4 mg/mL solution of chloramine-T (Sigma Chemical Co., St Louis, MO, USA) was added for 15 seconds with gentle agitation. This reaction was terminated by the addition of 50 μL of a 4.8 mg/mL solution of sodium metabisulfite (Sigma Chemical Co.) for 20 seconds with gentle agitation. The reaction mixture was then diluted with 200 μL 10% BSA and the resul-

tant mixture layered on a Bio-Gel P2 (Bio-Rad Labs) column (1.0 × 30 cm Econocolumn, Bio-Rad Labs) for NDP-MSH or on a Bio-Gel P6 (Bio-Rad Labs) column (1.0 × 50 cm Econocolumn, Bio-Rad Labs) for AGRP(87–132) for separation by size exclusion chromatography using 50 mM sodium phosphate buffer, pH 7.4 as column eluant. Fifteen drop fractions (approximately 500 μL) were collected into glass tubes containing 500 μL of 1% BSA. Each fraction was then counted on the Apex Automatic Gamma Counter (ICN Micromedic Systems Model 28023, with RIA AID software; Robert Maciel Associates, Inc.) to determine peak ^{125}I incorporation fractions.

Receptor-binding studies

Human embryonic kidney-293 cells stably expressing the WT and mutant receptors were maintained as described above. One day preceding the experiment, (0.6–0.8) × 10^6 cells per well were plated onto 12-well plates. The peptides NDP-MSH and hAGRP(87–132) were used to competitively displace the ^{125}I-radiolabeled peptides (150 000 c.p.m. per well) NDP-MSH and hAGRP(87–132), respectively. Dose–response curves (10^{-6} to 10^{-12} M) and IC_{50} values were generated and analyzed by non-linear least-squares analysis (55) and the PRISM program (version 4.0, GraphPad Inc.). The percentage total specific binding was determined based upon the non-specific values obtained using 10^{-6} M NDP-MSH or hAGRP(87–132) for the respective radiolabeled peptide. Each experiment was performed using duplicate data points and repeated in at least two independent experiments. The standard deviation errors of the mean were derived from the average percentage specific binding values from at least two independent experiments and using the PRISM program (v4.0, GraphPad Inc.). Statistical analysis was performed using a Student's *t*-test.

FACS analysis of wild-type and mutant Flag-tagged hMC4 receptors

Fluorescence-activated cell sorting (FACS) analysis of N-terminally Flag-tagged WT and mutant hMC4R was performed as described previously for the detection of the intracellular protein cyclo-oxygenase/prostaglandin synthase 2 ($COX2/PGS_2$) (56). The protocol was modified by using an allophycocyanin (APC)-conjugated anti-Flag monoclonal antibody (Prozyme, San Leandro, CA, USA) for both, cell surface and intracellular detection of the Flag-hMC4Rs. To detect cell surface expression of WT and mutant Flag-hMC4Rs, cells were incubated 45 min with APC-conjugated anti-Flag monoclonal antibody at a concentration of 1 μg/million cells. To detect the total (surface and intracellular) receptor expression cells were subsequently permeabilized with saponin buffer and stained an additional hour with the APC-conjugated anti-Flag monoclonal antibody. Unlabeled cells were used to set the background fluorescence staining for these analyses. BD Biosciences (San Jose, CA, USA) FACS Calibur flow cytometers were used to collect both stained cell percentages (surface and total) and mean fluorescence data were measured from a minimum of 10 000 collected events per sample. Experiments were repeated three independent times. The data are presented as the mean of the three experiments (±SEM). Statistical analysis was performed using a Student's *t*-test.

Three-dimensional hMC4R homology molecular modeling studies

Homology modeling of the hMC4R in the 'inactive' state in complex with AGRP (25), and in the 'active' state in complex with NDP-MSH (57), were derived based upon the crystal structure of rhodopsin (PDB-ID: 1 gzm) (58). The modeling of the active receptor conformation satisfied distance constraints resulting from modifications (disulfides, metal-binding clusters, hydrogen bonds between neighboring polar residues) that facilitate activation, which were applied in distance geometry calculations, as was described for modeling of the active conformation of the μ-opioid receptor (59). Based upon receptor mutagenesis and modeling results it has been previously proposed that for the MCRs, a β-hairpin is formed in the extracellular loop 1 (EL1; as in bacterial rhodopsins), and an additional short β-strand in the N-terminal segment is attached to EL3 by a disulfide bond between Cys^{40} and Cys^{279}, and another important disulfide bond Cys^{271}–Cys^{277} connects the EL3 to TM6 (25). Sequence alignment of MCRs and rhodopsin (25) assumes the disappearance of an α-aneurism [an insertion of an extra-residue(s) in an α-helix] in TM2 that is present in rhodopsin (60), but conservation of the α-aneurism in TM5 found in the rhodopsin crystal structure. In order to understand the results of the L250 mutations to Ala, Glu, Phe, Lys, Asn, Arg, and Gln the L250 side chain was substituted in the active and the inactive MC4R models to the corresponding side chains and the side chain rotamers were adjusted to avoid steric overlap and to provide favorable interactions (hydrogen bonds and van der Waals) with neighboring residues. Final energy minimization of all hMC4R models was performed using the CHARM (61) potential with $\varepsilon = 10$, and utilizing the adopted basic Newton-Raphson method (50-iterations). The models of the hMC4R in the 'active' and 'inactive' conformation can be found on the web site: http://mosberglab.phar.umich.edu/resources/index.php.

hMC4R residue numbering

Highly conserved GPCR residues in the TM domain of the hMC4R and other GPCRs are given two numbering schemes. First, residues are numbered according to their positions in the receptor amino acid sequence. Secondly, residues are numbered relative to the most conserved residue in the TM in which it is located (N1, N2). N1 refers to the TM number, and N2 refers to the position of the residue relative to the most conserved one with numbers decreasing towards the N-terminus and increasing toward the C-terminus. The most conserved residue is assigned the position number 50, e.g. P299 (7.50) and therefore D298 (7.49) and Y302 (7.53). This numbering scheme simplifies the identification of aligned residues in different GPCRs (62).

Animals

Seven adult male Sprague–Dawley rats (250–300 g, Charles Rivers) were utilized in these studies. All animals were treated humanely and protocols have been approved by the University of Florida Animal Care and Use Committee (IACUC). For the immunohistochemical study of hypothalamic arcuate neurons and their terminals, three rats were injected ICV with 120 mg colchicine in 10 μL 0.9% saline 24 h prior to cardiac perfusion. To increase the expression of AGRP, four rats were food deprived for 48 h and ICV injected with colchicine 24 h prior to kill to block axonal transport and increase the quantity of peptide in the neuronal cell bodies. Rodents were anesthetized i.p. with sodium pentobarbital and perfused via the ascending aorta with 0.9% sodium chloride solution (37 °C), followed by a mixture of formalin and picric acid (4% paraformaldehyde and 0.4% picric acid in 0.16 M phosphate buffer, pH 6.9, 37 °C). The brains were rapidly dissected out, immersed in the same fixative for 12 h, and subsequently rinsed in 0.1 M phosphate buffer, pH 7.4 and stored at −20 °C until utilized.

Immunohistochemistry

For double labeling of the α-MSH and AGRP proteins, floating sections were incubated sequentially in: (i) 1% BSA in PBS for 1 h; (ii) a mixture of two primary antibodies, sheep anti-α-MSH (diluted 1:2000; Chemicon, Temecula, CA, USA) and rabbit anti-AGRP (diluted 1:1000; Phoenix Pharmaceuticals, Belmont, CA, USA), which were diluted with 0.1% BSA and 5% Triton in PBS for 48 h; and (iii) two secondary antibodies, Cy3-conjugated donkey anti-sheep immunoglobulin G (IgG; diluted 1:100) and Cy2-conjugated donkey anti-rabbit IgG (diluted 1:100, Jackson Immunoresearch Laboratories, West Grove, PA, USA) in PBS for 24 h. The sections were rinsed in PBS for 30 min at room temperature between each incubation step. Sections were mounted on gelatin-coated slides and coverslipped. After processing, the sections were examined in a Zeiss (Germany) fluorescence microscope equipped by digital camera (Sony, Japan) using appropriate filters. For confocal microscopy, samples were recorded using a Zeiss LSM410 instrument. Approximately 30 optical slices of 0.5 μm thickness were sampled and combined to produce composite confocal images. All manipulations with contrast and illumination on color images are made using ADOBE PHOTOSHOP 6.0 software on a Windows PC.

Results

The primary sequences of the endogenous melanocortin agonists α-MSH, β-MSH, γ_2-MSH, and ACTH(1–24) (10,11), the synthetic melanocortin agonists NDP-MSH (63), MTII (19), and JRH887–9 (48), and the endogenous MC4R antagonist hAGRP(87–132) (8) used in this study are summarized in Table 2. Endogenous and synthetic agonists as well as the hAGRP(87–132) antagonist were included in this study to identify potential differences in ligand–receptor interactions between these structurally different compounds. To determine the molecular mechanism of constitutive activity of the L250Q

Peptide	Primary sequence
ACTH(1–24)	Ser-Tyr-Ser-Met-Glu-His-Phe-Arg-Trp-Gly-Lys-Pro-Val-Gly-Lys-Lys-Arg-Arg-Pro-Val-Lys-Val-Tyr-Pro
α-MSH	Ac-Ser-Tyr-Ser-Met-Glu-His-Phe-Arg-Trp-Gly-Lys-Pro-Val -NH_2
β-MSH	Ala-Glu-Lys-Lys-Asp-Glu-Gly-Pro-Tyr-Arg-Met-Glu-His-Phe-Arg-Trp-Gly-Ser-Pro-Pro-Lys-Asp
γ_2-MSH	Tyr-Val-Met-Gly-His-Phe-Arg-Trp-Asp-Arg-Phe-Gly
MTII	Ac-Nle-c[Asp-His-D-Phe-Arg-Trp-Lys]-NH_2
NDP-MSH	Ac-Ser-Tyr-Ser-Nle-Glu-His-D-Phe-Arg-Trp-Gly-Lys-Pro-Val-NH_2
JRH887–9	Ac-His-D-Phe-Arg-Trp-NH_2
hAGRP(87–132)	CVRLHESCLGQQVPCCDPCATCYCRFFNAFCYCRKLGTAMNPCSRT

Table 2: Primary sequences of agonists ACTH(1–24), α-MSH, β-MSH, γ_2-MSH (endogenous), MTII, NDP-MSH, JRH887–9 (synthetic) and the endogenous antagonist/inverse agonist hAGRP(87–132) used in this study

MSH, melanocyte-stimulating hormone; NDP, 4-norleucine-7-D-phenylalanine; ACTH, adrenocorticotropic hormone; AGRP, agouti-related protein.

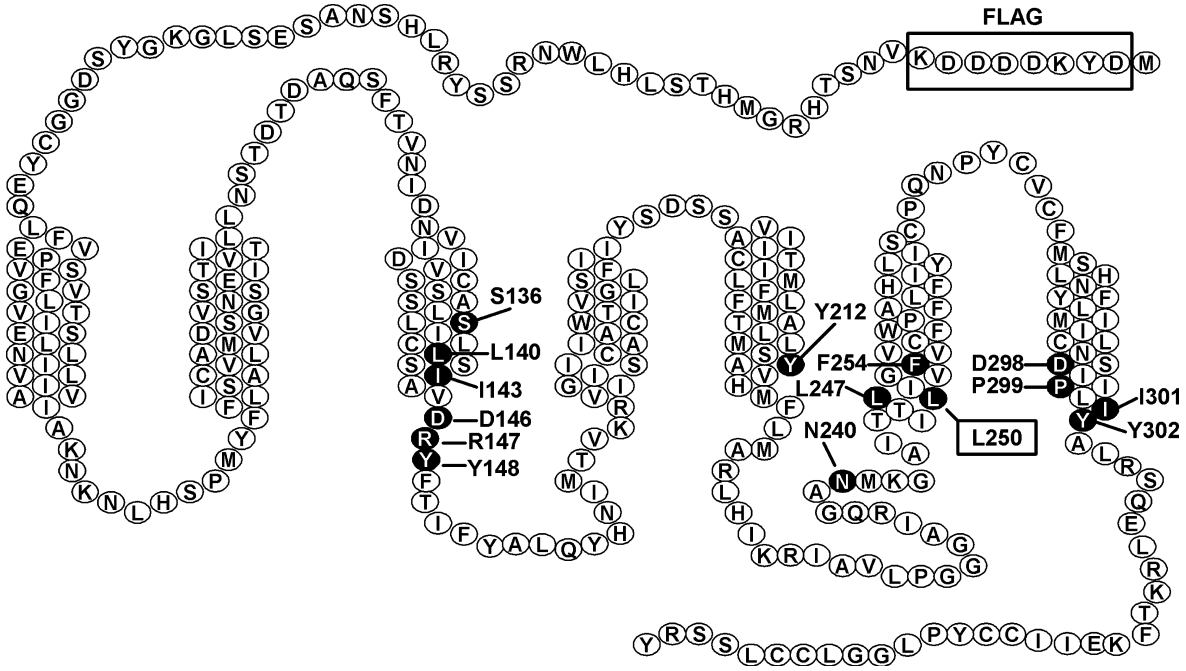

Figure 1: Two-dimensional model of the human Melanocortin-4 Receptor (hMC4R). Residues, depicted in black circles with white letters are involved in maintaining the active or inactive receptor conformation in L250 wild-type and mutant L250A, L250E, L250F, L250K, L250N, L250R, and L250Q hMC4Rs. The Flag-tag (highlighted in a square) was inserted downstream of the methionine start codon for immunocytochemical detection of the receptor.

hMC4R, *in vitro* mutagenesis was performed by mutating residue Leu250 (6.40) of the hMC4R to Ala, Glu, Phe, Lys, Asn, Arg, and Gln to determine requirements at this position for constitutive activation. Amino acids for receptor mutagenesis were systematically selected based upon differences in charge, hydrophobicity, aromaticity or size of the side chains of the amino acids. Figure 1 illustrates a two-dimensional (2D) model of the hMC4R and emphasizes the putative receptor residues implicated in 'activation' and maintaining the 'active' or 'inactive' receptor conformation in WT and mutant hMC4Rs.

Mutation of L250 does not affect ligand-binding affinity of the hMC4R

Table 3 summarizes the binding affinity (IC_{50}) values of NDP-MSH and hAGRP(87–132) at each of the seven modified hMC4Rs prepared in this study. For each radiolabeled peptide [^{125}I-NDP-MSH and ^{125}I-AGRP(87–132)] the respective non-iodinated peptide was used to competitively displace the labeled compound resulting in the binding affinity IC_{50} values. Mutation of the L250 (6.40) residue had no significant effect on NDP-MSH or hAGRP(87–132)-binding affinity, with the exception of hAGRP(87–132)-binding affinity at the L250N hMC4R. Ligand-binding affinity values of NDP-MSH and hAGRP(87–132) at the mutant receptors were essentially equipotent to the WT hMC4R, indicating that the L250 residue is not involved in ligand binding of either of these agonist or antagonist peptide ligands.

Agonist pharmacology observed at the wild-type and mutant hMC4Rs

Table 4 summarizes the mean agonist EC_{50} values (±SEM) of the peptides examined at the WT and mutant hMC4Rs. Figure 2 illustrates the functional agonist pharmacology of the WT control and the seven modified hMC4Rs generated in this study. The ligands

Table 3: Competitive binding affinity IC_{50} (nM) results at the wild-type and mutant hMC4Rs. Non-iodinated NDP-MSH and hAGRP(87–132) were used to competitively displace the corresponding ^{125}I-radiolabeled peptide

	Binding IC_{50} (nM)	
	NDP-MSH	hAGRP(87–132)
hMC4R	5.20 ± 0.59	24.7 ± 12.6
L250F	5.79 ± 2.14	4.56 ± 0.75
L250A	4.85 ± 0.87	5.68 ± 0.96
L250R	5.80 ± 0.52	34.0 ± 32.0
L250K	4.49 ± 0.87	14.3 ± 6.91
L250E	7.13 ± 8.30	14.0 ± 12.4
L250Q	4.17 ± 0.83	5.98 ± 0.53
L250N	5.38 ± 0.34	42.8 ± 15.5*

The indicated errors represent the standard deviation of the mean from at least two independent experiments performed in duplicate.
*$p < 0.05$ when compared with the wild-type hMC4R.
MSH, melanocyte-stimulating hormone; hMC4R, human Melanocortin-4 Receptor; NDP, 4-norleucine-7-D-phenylalanine; AGRP, agouti-related protein.

used in this experiment (Table 2) were selected to test and differentiate ligand–receptor interactions between the endogenous linear agonist peptides α-MSH, β-MSH, γ_2-MSH, and ACTH(1–24), the synthetic linear analog of α-MSH [NDP-MSH (63)], the cyclic synthetic agonist MTII (19), and the synthetic tetrapeptide JRH887–9 (48). At the WT hMC4R, the endogenous agonists α-MSH, β-MSH, and ACTH(1–24) and the synthetic tetrapeptide JRH887–9 all possessed essentially equipotent activity. The synthetic superpotent NDP-MSH and MTII agonist ligands possessed sub-nM potencies while the endogenous agonist γ_2-MSH possessed approximately 200-fold decreased potency when compared with the other endogenous agonists at the hMC4R. The α-MSH ligand was equipotent at the L250N hMC4Rs, slightly reduced potency at the L250F, L250K, L250E, and L250Q hMC4Rs, and significantly decreased potency at the L250A (39-fold) and L250R (65-fold) hMC4Rs, when compared with the WT control. When compared with the control hMC4R, the β-MSH agonist ligand possessed 15- to 33-fold decreased potency at the L250F, L250Q, and L250N hMC4Rs and significantly decreased potency at the L250A (43-fold), L250R (165-fold), L250K (70-fold), and L250E (41-fold). The endogenous γ_2-MSH agonist essentially possessed equipotent pharmacology at all the mutant hMC4Rs examined in this study. Relative to the WT hMC4R, ACTH(1–24) possessed 14- to 27-fold reduced potency at the L250F, L250E, L250Q, and L250N hMC4Rs, 55- to 58-fold decreased potency at the L250A and L250K hMC4Rs, respectively, and 220-fold reduced agonist potency at the L250R. The synthetic cyclic MTII peptide resulted in nearly equipotent WT activity at the L250F, L250E, L250Q, and L250N hMC4Rs, 14- to 18-fold decreased potency at the L250A and L250K hMC4Rs and 39-fold decreased potency at the L250R hMC4R. NDP-MSH possessed five- to seven-fold reduced potency at the L250F and L250Q hMC4Rs, 21- to 33-fold decreased potency at the L250A, L250E, and L250N hMC4Rs and 44- to 78-fold decreased potency at the L250K and L250R hMC4Rs, respectively. Interestingly, the tetrapeptide JRH887–9 (Ac-His-D-Phe-Arg-Trp-NH_2) possessed equipotent activity at the L250A, L250Q, and L250N hMC4Rs, and slightly reduced potency at the L250F, L250R, L250K, and L250E hMC4Rs. Overall, the structurally distinct endogenous and synthetic melanocortin agonist ligands

Table 4: Functional activity of melanocortin ligands at the wild-type and mutant hMC4 receptors

	Potency EC_{50}(nM)													
	α-MSH	Fold difference	β-MSH	Fold difference	γ_2-MSH	Fold difference	ACTH(1–24)	Fold difference	MTII	Fold difference	NDP-MSH	Fold difference	JRH887–9	Fold difference
hMC4R	0.88 ± 0.11	1	0.24 ± 0.07	1	170 ± 4.80	1	0.86 ± 0.04	1	0.017 ± 0.007	1	0.022 ± 0.006	1	0.72 ± 0.12	1
L250F	12.0 ± 2.58*	14	6.66 ± 1.88*	28	725 ± 88*	4	16.6 ± 2.74*	19	0.051 ± 0.003*	3	0.15 ± 0.003*	7	11.1 ± 3.57*	15
L250A	34.5 ± 12.7*	39	10.3 ± 3.44*	43	970 ± 207*	6	46.9 ± 12.0*	55	0.23 ± 0.06	14	0.52 ± 0.16*	24	6.25 ± 3.26	7
L250R	57.6 ± 16.3*	65	39.5 ± 5.32*	165	1480 ± 370	9	190 ± 18*	220	0.67 ± 0.007*	39	1.72 ± 0.30*	78	10.3 ± 0.95*	14
L250K	11.9 ± 6.94	13	16.7 ± 2.90*	70	530 ± 20*	3	49.9 ± 24.3	58	0.30 ± 0.05*	18	0.96 ± 0.20*	44	6.93 ± 0.98*	10
L250E	11.8 ± 3.17*	13	9.84 ± 0.99*	41	913 ± 560	5	23.5 ± 11.9	27	0.14 ± 0.035	8	0.73 ± 0.09*	33	3.76 ± 0.98*	5
L250Q	4.32 ± 1.10*	5	3.55 ± 1.67*	15	442 ± 24*	3	3.63 ± 0.82	4	0.034 ± 0.020	2	0.10 ± 0.02*	5	1.09 ± 0.29	2
L250N	1.55 ± 1.92	2	8.00 ± 0.91*	33	193 ± 63	1	13.2 ± 3.48*	15	0.054 ± 0.052	3	0.46 ± 0.16*	21	0.92 ± 0.31	1

EC_{50} values (nM; ±SEM) are derived from at least three independent experiments. The fold difference is calculated relative to the wild-type hMC4R.
*$p < 0.05$ when compared with the wild-type hMC4R.
MSH, melanocyte-stimulating hormone; hMC4, human Melanocortin-4 Receptor; NDP, 4-norleucine-7-D-phenylalanine; ACTH, adrenocorticotropic hormone.

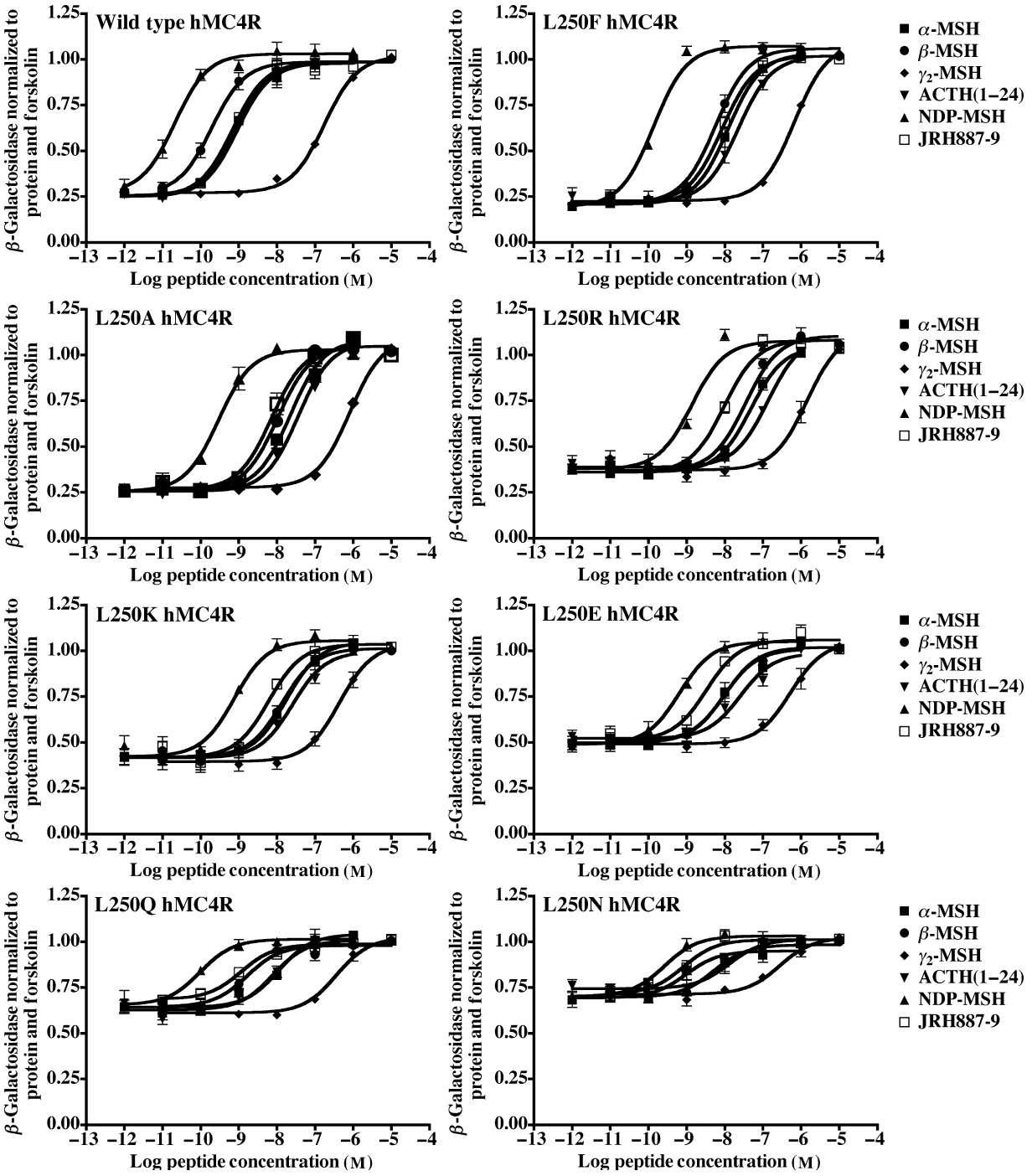

Figure 2: Agonist pharmacology of melanocortin ligands at the wild-type and mutant human Melanocortin-4 Receptor (hMC4Rs) stably expressed in human embryonic kidney-293 (HEK-293) cells.

examined in this study possess distinct pharmacologic profiles at the WT and mutant hMC4Rs.

L250X hMC4R constitutive activation

It has been previously demonstrated that the L250Q hMC4R polymorphism results in a constitutively active receptor that possesses increased cellular basal activity in the absence of agonist ligand (17,35,40). Figure 3 illustrates the basal activities observed for the stably expressed hMC4Rs examined in this study. Relative to the WT hMC4R, the L250F hMC4R possesses reduced basal activity ($p < 0.05$), the L250A hMC4R has equipotent basal activity, and the L250R, L250K, L250E, and L250N possess increased basal activity ($p < 0.01$). Transient transfection assays have been used to

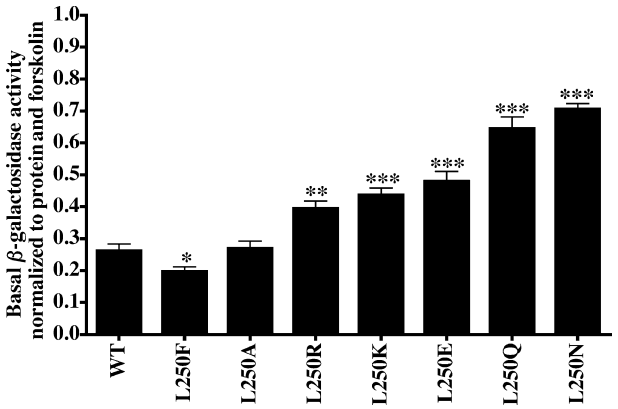

Figure 3: Basal levels of the wild-type and mutant human Melanocortin-4 Receptor (hMC4R) stably expressed in human embryonic kidney-293 (HEK-293) cells. Statistical analysis was performed using a Student's *t*-test where $^{*}p < 0.05$, $^{**}p < 0.01$, and $^{***}p < 0.001$.

ascertain if a receptor is a candidate as a constitutively active receptor versus possessing an artifact related to cell surface expression levels (49,53,64). Figure 4 summarizes the transient transfection of the hMC4Rs examined in this study and supports the hypothesis that the L250E, L250Q, and L250N hMC4Rs are constitutively active GPCRs. The L250K hMC4R possesses increased basal activity with increasing DNA concentrations when compared with the WT, L250F, L250A, and L250R hMC4Rs and thus may also be considered as constitutively active.

Cell surface expression of wild-type and mutant hMC4 receptors

A decrease in relative cell surface expression of the receptor using FACS has previously been proposed as a mechanism of impaired receptor function of the constitutively active mutant L250Q hMC4R (35,40). Therefore, we determined the cell surface expression of the WT and mutant hMC4Rs using the N-terminal Flag-hMC4Rs and FACS analysis quantification. Figure 5 summarizes the percentage of cell surface expression of the WT and mutant hMC4Rs stably expressed in HEK-293, relative to the WT hMC4R. Cell surface and total receptor expression of the WT hMC4R were defined as 100%. In Table 5, the receptor cell surface expression of WT and mutant hMC4Rs are compared with the functional activity of α-MSH at those receptors and their status as constitutively active receptors. The mutant hMC4Rs L250A, L250F, and L250R possessed receptor cell surface expression levels of 57%, 46%, and 52%, relative to the WT hMC4R. The L250K mutant hMC4R which shows intermediate and constitutive activation and possessed cell surface expression levels of 58% relative to the WT hMC4R. The constitutively active L250E, L250N, and L250Q mutant hMC4Rs (Figure 3) possessed cell surface expression levels of 66%, 54% and 72%, respectively, relative to the WT hMC4R (Figure 5, Table 5). Thus, there does not appear to be a correlation between the endogenous agonist α-MSH potency and receptor cell surface expression levels.

hAGRP(87–132) antagonist and inverse agonist pharmacology at the wild-type and mutant hMC4Rs

Table 6 summarizes the pA_2 values (±SD) of hAGRP(87–132) at the WT and mutant hMC4Rs. Figure 6 illustrates the inverse agonist and antagonist curves of the hAGRP(87–132) ligand at the hMC4Rs examined in this study. The pharmacologic profile of the hAGRP (87–132) ligand at the WT hMC4R presented herein is consistent with previously published results that this ligand possesses inverse agonist activity at both mouse and human MC4Rs (26,27). Varying degrees of hAGRP(87–132) inverse agonist activity is observed at the L250K, L250E, L250Q, and L250N hMC4Rs, with the most pronounced effect observed at the L250N hMC4R. These data support the hypothesis that these latter hMC4Rs are constitutively active receptors (Figures 3 and 4). Interestingly, the hAGRP(87–132) antagonist is equipotent at all the receptors examined in this study within independent experiments and the error, with the exception

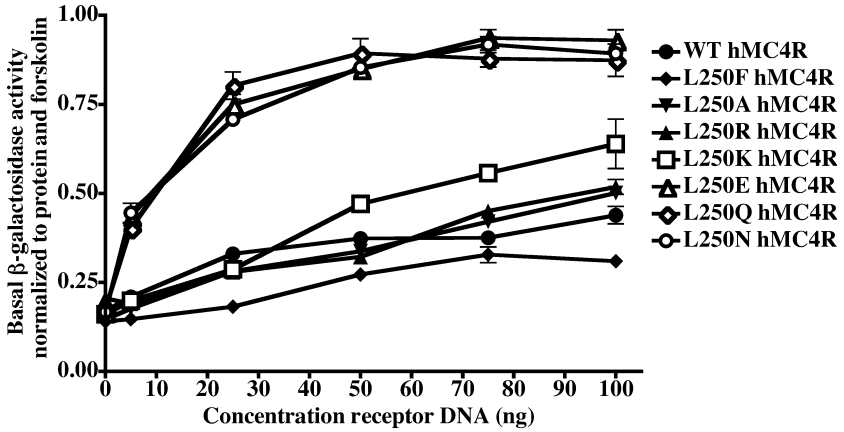

Figure 4: Transient transfection bioassay: increasing amounts of wild-type and mutant human Melanocortin-4 Receptor (hMC4R) DNA were transiently transfected into human embryonic kidney-293 (HEK-293) cells as described under Materials and Methods. The L250E, L250Q, and L250N mutants result in increased basal activity with increasing amount of DNA and are therefore indicative of possessing constitutive activity in the absence of an agonist ligand. The wild-type hMC4R, the L250R, L250A, and L250F hMC4R mutants do not result in significantly increased basal activity and either lack or show very low levels of constitutive activation. The mutant L250K hMC4R shows moderate constitutive activity.

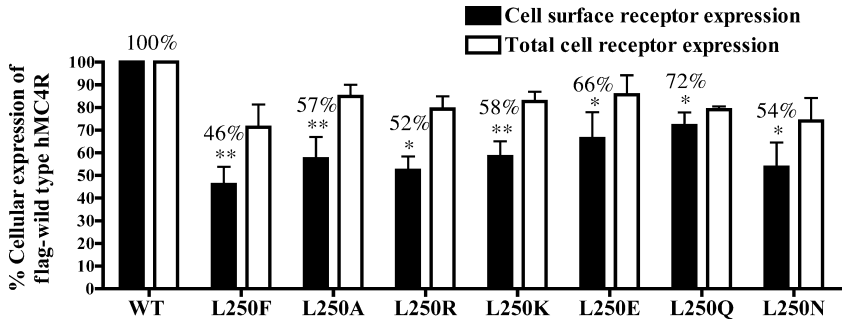

Figure 5: Comparison of the wild-type and mutant human Melanocortin-4 Receptor (hMC4R) cell surface and total receptor expression levels using fluorescent-activated cell sorting (FACS). Cell surface and total receptor expression of the wild-type hMC4R were defined as 100% for comparative purposes. The values listed indicate the average of the mean from three independent experiments and the error bars represent the standard error of the mean. Statistical analysis was performed using a Student's *t*-test with statistical significance indicated as *$p < 0.05$ and **$p < 0.01$.

Table 5: Comparison of receptor cell surface expression with the functional activity of the endogenous ligand α-MSH and the level of constitutive activation of mutant and wild type hMC4 receptors

	Receptor cell surface expression (%)	α-MSH potency (EC_{50} in nM)	Fold difference	Constitutive activation
hMC4R	100	0.88 ± 0.11	1	No
L250F	46 ± 9.6*	12.0 ± 2.58*	14	No
L250A	57 ± 9.6*	34.5 ± 12.7*	39	No
L250R	52 ± 6.1*	57.6 ± 16.3*	65	No
L250K	58 ± 6.8*	11.9 ± 6.94	13	Intermediate
L250E	66 ± 11.6*	11.8 ± 3.17*	13	Yes
L250Q	72 ± 5.8*	4.32 ± 1.10*	5	Yes
L250N	54 ± 10.9*	1.55 ± 1.92	2	Yes

Receptor cell surface expression of the wild-type hMC4R was set to 100%. EC_{50} values (nM; ±SEM) are derived from at least three experiments performed in duplicate. The fold difference in EC_{50} values is calculated relative to the wild-type hMC4R.

*$p < 0.05$ when compared with the wild-type hMC4R.

MSH, melanocyte-stimulating hormone; hMC4, human Melanocortin-4 Receptor.

Table 6: Functional activity of the antagonist hAGRP(87–132) at the wild-type and mutant hMC4Rs

	Antagonist pA_2 value [hAGRP(87–132)]
hMC4R	8.20 ± 0.007
L250F	8.64 ± 0.04*
L250A	8.12 ± 0.22
L250R	7.64 ± 0.35
L250K	8.24 ± 0.01
L250E	8.27 ± 0.50
L250Q	8.53 ± 0.64
L250N	9.13 ± 0.97

pA_2 values (±SD) are derived from at least two independent experiments performed in duplicate.

*$p < 0.05$ when compared with the wild-type human Melanocortin-4 Receptor (hMC4R).

hMC4R, human Melanocortin-4 Receptor; AGRP, agouti-related protein.

of the L250F ($p < 0.05$). However, at the L250N hMC4R it possess a ninefold enhanced potency based on comparison of K_i values, where $K_i = -\log pA_2$ (52) (Table 6).

Dual label rat hypothalamic immunohistochemistry

The endogenous melanocortin agonist α-MSH and antagonist AGRP have been reported to be expressed at the mRNA level in the arcuate nucleus (ARC) of the hypothalamus in rodents and primates (65,66). Additionally, both the α-MSH and AGRP proteins are expressed in distinct neuronal populations within the ARC and project to brain nuclei that express melanocortin receptor (MC3R and MC4R) mRNA. Because AGRP has been identified to function as an inverse agonist of the MC4R using *in vitro* heterologous cell lines, we utilized a fasted rat model in attempts to identify any physiologic data that might support the hypothesis that AGRP might function as an inverse agonist in the hypothalamus as well. Confocal microscopy of dual-labeled immunohistochemical hypothalamic coronal sections of fasted and colchicines-treated rats demonstrates the expression of α-MSH and AGRP in different neuronal populations of the ARC (Figure 7A), consistent with previous results observed for singly labeled samples (65,66). Furthermore, in agreement with previous studies (65,66), we observed α-MSH and AGRP high-density networks of labeled neuronal fibers in various hypothalamic nuclei of the brain and within the macrostructure of the paraventricular nucleus (PVN; Figure 7). Interestingly, as illustrated in Figure 7B, distinct subnuclei neuronal populations of the PVN appear to express only hAGRP (green) or α-MSH (red). These data support the hypothesis that hAGRP may possess additional physiologic roles such as inverse agonism, in addition to its well recognized role as an MC3R and MC4R competitive antagonist of the endogenous α-MSH ligand. Furthermore, within the ARC it appears that AGRP-expressing fibers (green) interact with the POMC-expressing neurons (red; Figure 7C,D), to function in an autoregulatory feedback mechanism, whereas the AGRP-expressing neurons are devoid of POMC-expressing fiber contacts (Figure 7E). These data are consistent with previous reports demonstrating neuropeptide Y (NPY)-expressing neurons that co-express AGRP synapse on POMC-expression neurons (67). These experiments provide physiologic data

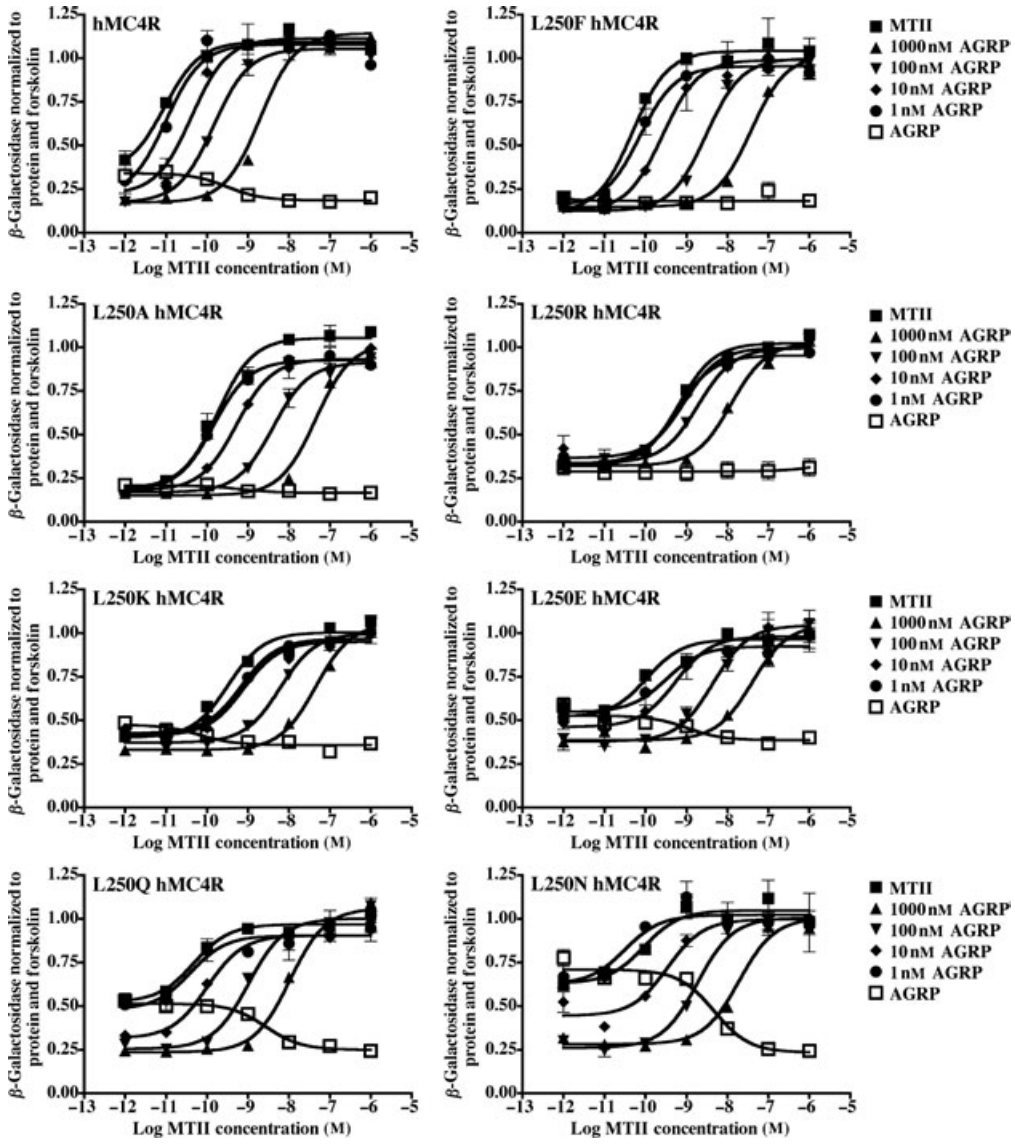

Figure 6: Antagonist and inverse agonist pharmacology of hAGRP(87–132) at the wild-type and mutant human Melanocortin-4 Receptor (hMC4Rs) stably expressed in human embryonic kidney-293 (HEK-293) cells. The corresponding pA_2 values were generated using the Schild analysis method.

supporting the hypothesis that the endogenous AGRP ligand appears to possess additional physiologic functions than simply acting as a competitive antagonist of α-MSH at the centrally expressed MCRs. These additional physiologic functions may include autoregulation of POMC-expressing neuronal homeostasis and perhaps as an inverse agonist in subnuclei that are not innervated by the α-MSH agonist.

Discussion

Herein, we investigated not only the mechanism by which a naturally occurring L250Q mutant hMC4R (found in a severely obese woman) might contribute to the obesity development in this patient, but also the molecular mechanism and requirements responsible for constitutive receptor activation of the hMC4R. The melanocortin system, in particular the MC4R, plays a major physiologic role in obesity, satiety, and energy homeostasis in both humans and rodents (12–16,28,29). Since the first discovery of naturally occurring mutations in the hMC4R in severely obese patients in 1998 (28,29), a large number of polymorphisms in the MC4R have been discovered in morbidly obese children and adults (17,18,28–47). However, the molecular mechanisms by which these mutations alter receptor function and subsequently may cause obesity are currently being unraveled by several research groups (17,18,35,42,47). Multiple studies have been undertaken to characterize these mutant receptors functionally *in vitro* using heterologous cell lines transiently or stably expressing polymorphic hMC4Rs. Current hypotheses for hMC4R polymorphic receptor malfunction associated with an obese human phenotype include modified potency of the endogenous melanocortin agonists, truncated or structurally non-functional receptors, and decreased cell surface expression and intracellular

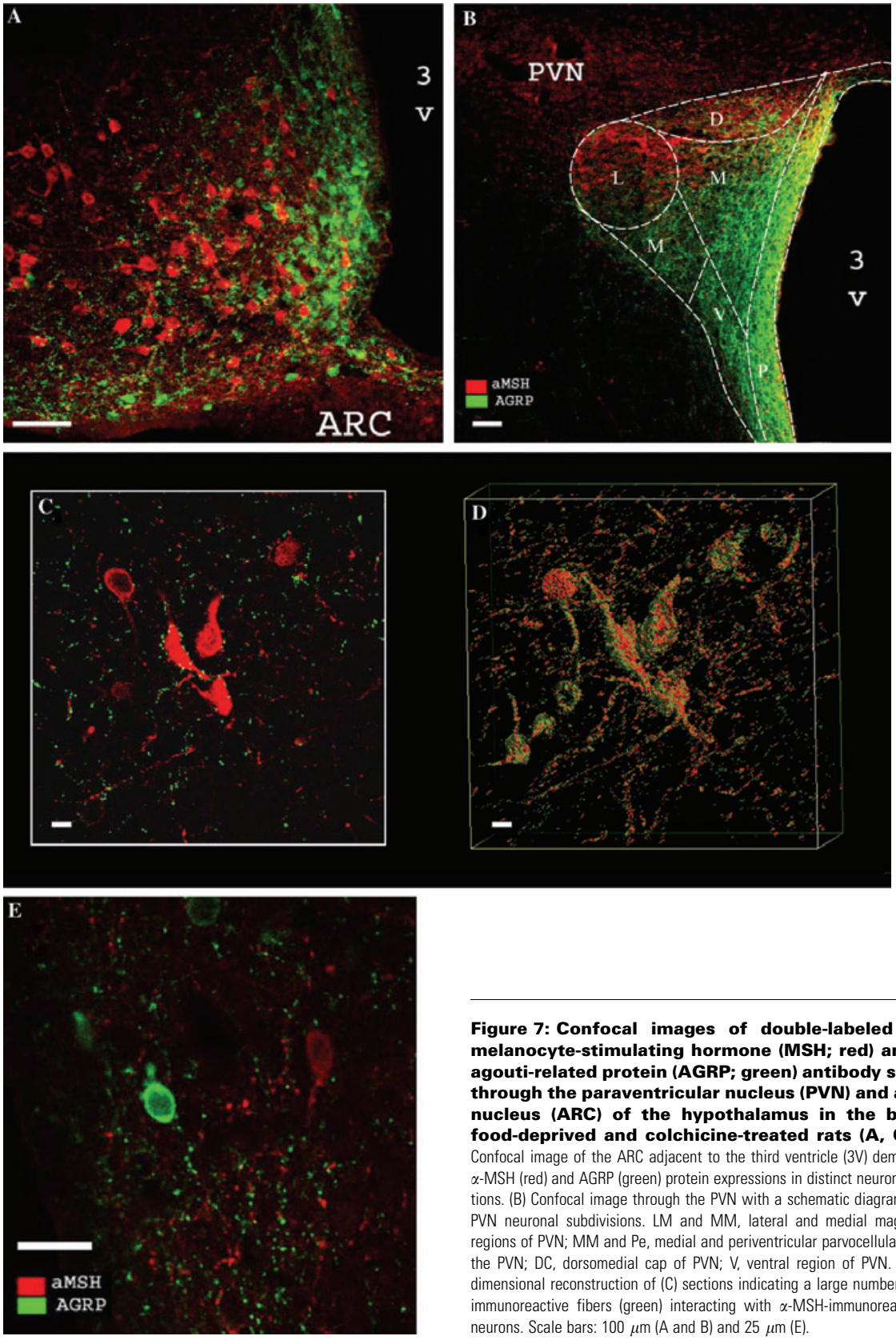

Figure 7: Confocal images of double-labeled anti-α-melanocyte-stimulating hormone (MSH; red) and anti-agouti-related protein (AGRP; green) antibody sections through the paraventricular nucleus (PVN) and arcuate nucleus (ARC) of the hypothalamus in the brain of food-deprived and colchicine-treated rats (A, C–E). (A) Confocal image of the ARC adjacent to the third ventricle (3V) demonstrating α-MSH (red) and AGRP (green) protein expressions in distinct neuronal populations. (B) Confocal image through the PVN with a schematic diagram showing PVN neuronal subdivisions. LM and MM, lateral and medial magnocellular regions of PVN; MM and Pe, medial and periventricular parvocellular region of the PVN; DC, dorsomedial cap of PVN; V, ventral region of PVN. (D) Three-dimensional reconstruction of (C) sections indicating a large number of AGRP-immunoreactive fibers (green) interacting with α-MSH-immunoreactive (red) neurons. Scale bars: 100 μm (A and B) and 25 μm (E).

retention in the endoplasmic reticulum (17,18,28–47). However, none of the above proposed mechanisms singly could explain the mechanism by which the constitutively active L250Q mutant MC4R may be involved in obesity development in humans. Binding affinities of the melanocortin agonist NDP-MSH and the antagonist/inverse agonist hAGRP(87–132) ligands to the L250Q polymorphic receptor hMC4R are equipotent to the WT hMC4R (Table 3), which indicates that this L250 (6.40) residue is not important for ligand binding or the molecular recognition aspects of ligand–receptor interactions. A decrease in relative cell surface expression using FACS has been proposed as a mechanism of impaired receptor function of the mutant L250Q hMC4R (35,40), but this alone (Figure 5,Table 5) in the context of a heterozygote genotype of a morbidly obese female patient with a body mass index (BMI) of 59 (17), does not correlated well with a constitutively active hMC4R, which based upon current research would be hypothesized to result in a lean phenotype. This rationale led us to the hypothesis that AGRP may act as inverse agonist at this constitutively active polymorphic L250Q hMC4R, thus decreasing the high basal cAMP levels. Herein, we have demonstrated that hAGRP(87–132) is able to dose-dependently suppress basal activity of the L250Q hMC4R to levels similar to the basal activity of the WT hMC4R (Figure 6). The identification of AGRP as inverse agonist (25–27) provided evidence that AGRP may play an alternative role in energy homeostasis, in addition to competitive antagonism of α-MSH (26,27). Furthermore, AGRP could have a physiologic function in and of itself, thus acting both independently and in concert with the POMC-derived melanocortin agonist α-MSH (26,27). The endogenous AGRP ligand is expressed in neurons of the ARC (Figure 7) in the hypothalamus of the brain and is implicated in the regulation of energy homeostasis (8,21). These AGRP-containing neurons are near the POMC-containing ARC neurons that produce the MCR agonist α-MSH (68–72). It has been shown that during chronic food restriction, mRNA levels encoding the orexigenic peptide AGRP are increased (8,21) and mRNA levels encoding the prohormone POMC of the anorexigenic peptide α-MSH are decreased in the hypothalamus (73,74). It has also been suggested that regulation of MC4R signaling in the hypothalamus could be mediated primarily by changes in AGRP expression rather than POMC, the precursor of α-MSH (69). Based upon these data, we hypothesize that increased basal cAMP levels, as observed at the constitutively active L250Q hMC4R mutant receptor could mimic chronic food restriction and subsequently trigger increased AGRP release from nearby situated AGRP neurons (Figure 7). Thus, AGRP could decrease the basal activity of the receptor by acting as inverse agonist and modify the POMC-derived agonist homeostasis in adjoining ARC neurons (Figure 7), resulting in a counterregulatory action of increased appetite and hyperphagia which in turn may lead to the development of obesity in this patient. Additionally, it has been demonstrated that AGRP can cause a long-term orexigenic effect, which completely blocks the anorectic effect of the synthetic MTII agonist (23). This observation would support the hyperphagia and obesity observed in the L250Q patient. However, the extent and the physiologic mechanism by which AGRP and the constitutively active L250Q mutant hMC4R contribute to the obesity development in the 'L250Q phenotype' remain to be experimentally verified using *in vivo* physiologic studies. An additional physiologic mechanism may be that the constitutive activation of L250Q is accompanied by the constitutive desensitization of the L250Q hMC4R and its sequestration into the internal vesicles. This would decrease the number of functional receptors on the neuronal membrane. Similar effects have been previously observed for a number of constitutively active mutants of GPCRs, such as mutant β-adrenoreceptors (75) and rhodopsin mutants causing congenital night blindness (76). Again, further studies need to be performed to examine this possible alternative mechanism.

Hypothesized molecular mechanism of the constitutively active L250Q hMC4R

To understand the putative molecular mechanisms by which the L250Q hMC4R human polymorphism results in a constitutively active GPCR, we systematically mutated the L250 residue to Ala, Glu, Phe, Lys, Asn, Arg, and Gln in order to determine the requirements at this position that are necessary for hMC4R constitutive activation. Amino acids for receptor mutagenesis were selected due to differences in hydrophobicity, charge, size, length of the side chain, and aromaticity to test our hypothesis that this L250Q hMC4R modifies the different 'active' and 'inactive' receptor populations of the GPCR ternary complex model, specifically via intramolecular interactions with TM3 and TM7 residues. We observed that L250N, L250Q, and L250E hMC4Rs possessed significantly increased basal activity ($p < 0.001$) when compared with the WT control with L250N > L250Q > L250E (Figure 3). Based upon the transient transfection experiment (Figure 4), the L250K hMC4R possessed moderate constitutive activation and the L250F, L250A, and L250R hMC4Rs were not constitutively active. Competitive antagonists can act as inverse agonists at constitutively active GPCRs (77,78) and indeed, we have observed inverse agonist activity of the hAGRP(87–132) at the constitutively active L250E, L250Q, and L250N hMC4Rs (Figure 6). At the non-constitutively active L250F, L250A, and L250R mutant hMC4Rs, hAGRP(87–132) possessed normal competitive antagonist activity with little observable inverse agonist activity.

The hMC4R mutagenesis results observed in the study presented herein, might be explained using theoretical three-dimensional (3D) homology molecular models of an active (agonist-bound) and an inactive (antagonist-bound) conformation of the hMC4R. The models used herein have been developed based on a number of experimental constraints collected for different GPCRs and MC4R ligand and receptor mutagenesis studies (25,57). Numerous experimental studies provide evidence for the conformational changes during activation of the receptors, such as side chain rearrangement leading to the disruption of inactivating intermolecular constraints, rotation, and shift of TM6 and some adjustment of all other helices (79–81). The major difference between models of the 'active' and 'inactive' hMC4R state is the putative large movement of the TMs creating a water-filled cavity between the intracellular segments of TMs 6, 3, and 7, and the rearrangement of hydrogen bond networks between the TMs (79,81,82). For example, the hydrogen bond network between residues D146 (3.49), R147 (3.50), and N240 (6.30) in the inactive state model of the hMC4R is replaced by a hydrogen bond system between residues R147 (3.50), Y212 (5.58), and Y302 (7.53) in the model of the active state (Figure 8) (25,57). In fact, the essential role of the side chain interactions of Asp/Glu (3.49), Arg (3.50), Tyr (5.58), and Tyr (7.53) during GPCR activation have been experimentally supported (79,81,83,84).

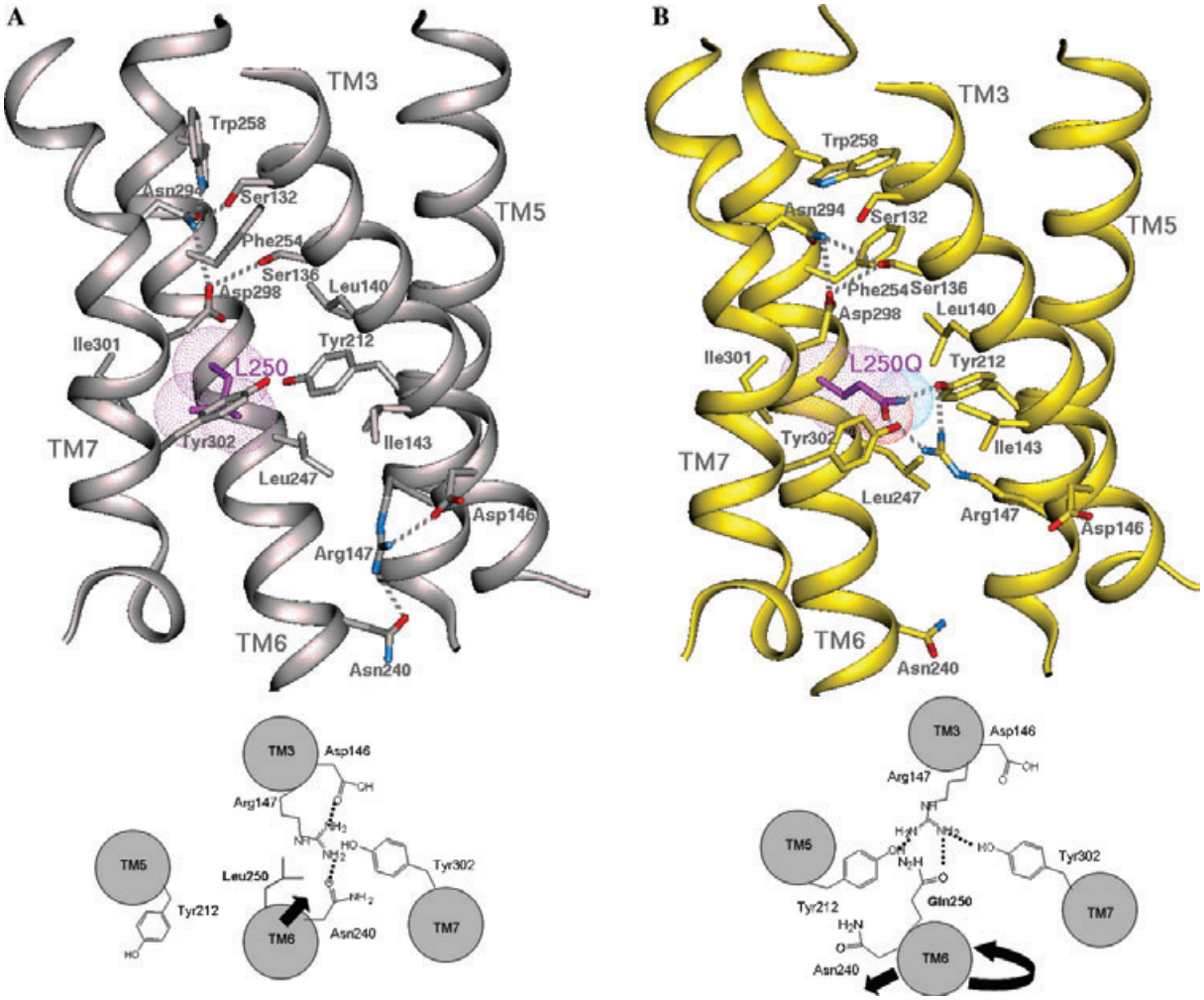

Figure 8: Comparison of three-dimensional homology human Melanocortin-4 Receptor (hMC4R) models of the wild-type hMC4R (A, gray) and L250Q hMC4R (B, yellow) mutants in the putative 'inactive' and 'active' receptor conformations, respectively. Homology modeling of the hMC4R in the 'inactive' state in complex with agouti-related protein (AGRP) and in the 'active' state in complex with 4-norleucine-7-D-phenylalanine melanocyte-stimulating hormone (NDP-MSH) was based on the crystal structure of rhodopsin and was carried out as described under Materials and Methods. The fragments of transmembrane (TMs) 3, 5, 6, and 7 are shown as ribbon, the mutated L250 residue (purple) and several residues surrounding the mutated residue and forming hydrogen-bonding interactions are shown by licorice. Schematic representations of four TM helices with mutated and some interacting residues are shown in the bottom part of the picture.

Our theoretical modeling studies reveal a putative significant change in the environment of the L250 residue during activation of hMC4R. In the model of the 'inactive' receptor state L250 (6.40) occupies a hydrophobic site between TMs 3, 6, and 7 formed by residues L140 (3.43), I143 (3.46), L247 (6.37), F254 (6.44), I301 (7.52), Y302 (7.53). In the 'active' state model the space between TM3 and TM6 is enlarged and the L250 side chain faces the water-filled cavity, while retaining weakened hydrophobic contacts with TM7. The substitution of L250 by the bulky aromatic side chain of Phe may increase the hydrophobic interactions between TMs 3, 6, and 7 and therefore may be advantageous for keeping the receptor in the 'inactive' conformation (Figure 8A). In contrast, the L250 substitution by polar side chains of Asn, Gln, and Glu (but not Lys and Arg) would not only destabilize the hydrophobic interactions suitable for the 'inactive' state, but also may be involved in the formation of interhelical hydrogen bonds with R147 (3.49) and Y212 (5.58) appropriate for the 'active' receptor state (Figure 8B). Such hydrogen bond interactions that stabilize the 'active' receptor state would explain the increased constitutive activity of the L250N, L250Q, and L250E mutants of hMC4R. A similar mechanism may account for the observed constitutive activity of M257N, M257Y, and M257S mutants of rhodopsin (86). Therefore, L250N, L250Q, and L250E hMC4R mutations represent the rare case of constitutively active mutants that are caused by the stabilization of the 'active' conformation rather than by destabilization of the 'inactive' receptor state. Another example of a mutation that may lock the receptor in the active conformation has been recently observed for the L457R mutant of lutropin receptor (85) in which the active conformation is stabilized by formation of a salt bridge between residues R457 in TM3 (3.43) and D578 in TM6 (6.44).

Changes in the potency of different agonist ligands at the different L250X hMC4R mutants may be related to the continuum of receptor substates that has been hypothesized to be formed in the presence of different ligands (86–88). Some of the activated receptor substates are appropriate for the interaction with specific G-proteins, kinases, β-arrestins or other proteins interacting with activated receptors (89). The results of this study demonstrating increased basal activity of L250N, L250Q, and L250E (6.40) mutants of the hMC4R, in addition to previous reports of constitutive activity of corresponding M257N and M257Y (6.40) mutants in rhodopsin (90) indicate that residue 6.40 may have an important structural role for GPCR activation, regulating the position of TM6 relative to TM3 and TM7. The different lengths of the Glu and Asn side chains and the putative different strength of Glu and Gln interactions with R147 (3.50) may favor formation of several active substates characterized by dissimilar positions of TM6 relative to the rest of the receptor (59). Indeed, the L250N, L250Q, and L250E hMC4R mutants demonstrated different levels of increased basal activity (Figures 3 and 4) and of agonist potency changes (Table 4). The L250N mutant, with the highest constitutive activity, probably has a side chain length more suitable for the formation of a hydrogen bond with R147 (3.50) and for the placement of TM6 that provides most effective activation of G-protein. The L250N, L250Q, and L250E mutants may also be constitutively phosphorylated at different levels and to a certain extent may lead to long-term desensitization and downregulation of the receptor number at the cell surface. However, this latter speculation remains to be experimentally verified. The presence of the polar, basic side chains of K250 or R250 putatively decrease the hydrophobic interactions placing TMs 3, 6, and 7 in the 'inactive' receptor, but do not provide the hydrogen bonding interactions necessary for stabilizing the 'active' state. Therefore, the basal activity of the corresponding L250K and L250R mutants were relatively low. Moreover, the R250 side chain may form hydrogen bonds with S136 (3.39), D298 (7.49), and Y302 (7.53), appropriate for the 'inactive-like' rather then for the 'active-like' receptor conformation. This could explain the minimal level of constitutive activation of the L250R mutant and the decreased agonist potency in this case (Table 4). The small side chain of the L250A mutant probably destabilizes both 'active' and 'inactive' states, thus causing decreased potency of agonists. The bulky L250F side chain can reinforce TM6–7 interactions and impede separation of these helices upon receptor activation, which would decrease the amount of activated receptors. This would explain the reduced potency of agonists at the mutant L250F hMC4R. On the other hand, the smaller hydrophobic side chain of L250 in the WT hMC4R may have smaller stabilization effect on the inactive conformation, leading to a higher population of activated receptors upon agonist binding. These mechanistic speculations remain to be experimentally verified; however, based upon the data generated in this study, these speculations provide specific molecular hypotheses to be further examined.

Conclusions and Future Directions

In conclusion, by performing receptor mutagenesis and creating seven hMC4R mutations at position 250 (6.40), we have identified requirements for receptor stimulation of the hMC4R and residues putatively involved in hMC4R activation. We propose that the hMC4R residue L250 is playing a key role in switching the hMC4R from the 'active' to the 'inactive' receptor conformation. These results can be used to gain further insight into the receptor activation mechanism of GPCRs and can be applied to other GPCR systems in order to stabilize the active receptor state for further crystallographic studies. We have generated experimental evidence that AGRP functions as an *in vitro* inverse agonist at the constitutively active L250Q hMC4R, and physiologic data supporting the hypothesis for additional functional roles for AGRP besides a competitive antagonist in the brain. These data taken together support the hypothesis that in addition to reduced cell surface expression, inverse agonist activity of the hAGRP antagonist may provide the molecular basis to explain the unanticipated phenotype of the obese phenotype associated with the constitutively active L250Q hMC4R.

Acknowledgments

The authors are grateful to Dr Andrei Lomize for helpful discussions. This study has been supported by NIH grants RO1DK063974, RO1DK57080, RO1DK064250, and an American Diabetes Association Research Award (CHL). Grant DA03910 from the National Institute on Drug Abuse (H.I.M) and the University of Michigan Upjohn Research Award G003878 (I.P.).

References

1. Chhajlani V., Wikberg J.E. (1992) Molecular cloning and expression of the human melanocyte stimulating hormone receptor cDNA. FEBS Lett;309:417–420.
2. Mountjoy K.G., Robbins L.S., Mortrud M.T., Cone R.D. (1992) The cloning of a family of genes that encode the melanocortin receptors. Science;257:1248–1251.
3. Mountjoy K.G., Mortrud M.T., Low M.J., Simerly R.B., Cone R.D. (1994) Localization of the melanocortin-4 receptor (MC4-R) in neuroendocrine and autonomic control circuits in the brain. Mol Endocrinol;8:1298–1308.
4. Roselli-Rehfuss L., Mountjoy K.G., Robbins L.S., Mortrud M.T., Low M.J., Tatro J.B., Entwistle M.L., Simerly R.B., Cone R.D. (1993) Identification of a receptor for gamma melanotropin and other proopiomelanocortin peptides in the hypothalamus and limbic system. Proc Natl Acad Sci U S A;90:8856–8860.
5. Gantz I., Konda Y., Tashiro T., Shimoto Y., Miwa H., Munzert G., Watson S.J., DelValle J., Yamada T. (1993) Molecular cloning of a novel melanocortin receptor. J Biol Chem;268:8246–8250.
6. Gantz I., Miwa H., Konda Y., Shimoto Y., Tashiro T., Watson S.J., DelValle J., Yamada T. (1993) Molecular cloning, expression, and gene localization of a fourth melanocortin receptor. J Biol Chem;268:15174–15179.
7. Gantz I., Shimoto Y., Konda Y., Miwa H., Dickinson C.J., Yamada T. (1994) Molecular cloning, expression, and characterization of a fifth melanocortin receptor. Biochem Biophys Res Commun;200:1214–1220.
8. Ollmann M.M., Wilson B.D., Yang Y.K., Kerns J.A., Chen Y., Gantz I., Barsh G.S. (1997) Antagonism of central melanocortin receptors in vitro and in vivo by agouti-related protein. Science;278:135–138.
9. Lu D., Willard D., Patel I.R., Kadwell S., Overton L., Kost T., Luther M., Chen W., Woychik R.P., Wilkison W.O. et al. (1994) Agouti protein is an antagonist of the melanocyte-stimulating-hormone receptor. Nature;371:799–802.
10. Eipper B.A., Mains R.E. (1980) Structure and biosynthesis of pro-ACTH/endorphin and related peptides. Endocr Rev;1:1–26.
11. Smith A.I., Funder J.W. (1988) Proopiomelanocortin processing in the pituitary, central nervous system and peripheral tissues. Endocr Rev;9:159–179.
12. Butler A.A., Kesterson R.A., Khong K., Cullen M.J., Pelleymounter M.A., Dekoning J., Baetscher M., Cone R.D. (2000) A unique metabolic syndrome causes obesity in the melanocortin-3 receptor-deficient mouse. Endocrinology;141:3518–3521.

13. Chen A.S., Marsh D.J., Trumbauer M.E., Frazier E.G., Guan X.M., Yu H., Rosenblum C.I., Vongs A., Feng Y., Cao L., Metzger J.M., Strack A.M., Camacho R.E., Mellin T.N., Nunes C.N. et al. (2000) Inactivation of the mouse melanocortin-3 receptor results in increased fat mass and reduced lean body mass. Nat Genet;26:97–102.
14. Fan W., Boston B.A., Kesterson R.A., Hruby V.J., Cone R.D. (1997) Role of melanocortinergic neurons in feeding and the agouti obesity syndrome. Nature;385:165–168.
15. Krude H., Biebermann H., Luck W., Horn R., Brabant G., Gruters A. (1998) Severe early-onset obesity, adrenal insufficiency and red hair pigmentation caused by POMC mutations in humans. Nat Genet;19:155–157.
16. Huszar D., Lynch C.A., Fairchild-Huntress V., Dunmore J.H., Fang Q., Berkemeier L.R., Gu W., Kesterson R.A., Boston B.A., Cone R.D., Smith F.J., Campfield L.A., Burn P., Lee F. (1997) Targeted disruption of the melanocortin-4 receptor results in obesity in mice. Cell;88:131–141.
17. Vaisse C., Clement K., Durand E., Hercberg S., Guy-Grand B., Froguel P. (2000) Melanocortin-4 receptor mutations are a frequent and heterogeneous cause of morbid obesity. J Clin Invest;106:253–262.
18. Farooqi I.S., Keogh J.M., Yeo G.S., Lank E.J., Cheetham T., O'Rahilly S. (2003) Clinical spectrum of obesity and mutations in the melanocortin 4 receptor gene. N Engl J Med;348:1085–1095.
19. Al-Obeidi F., Castrucci A.M., Hadley M.E., Hruby V.J. (1989) Potent and prolonged acting cyclic lactam analogues of α-melanotropin: design based on molecular dynamics. J Med Chem;32:2555–2561.
20. Hruby V.J., Lu D., Sharma S.D., Castrucci A.M.L., Kesterson R.A., Al-Obeidi F.A., Hadley M.E., Cone R.D. (1995) Cyclic lactam α-melanotropin analogues of Ac-Nle^4-c[Asp^5, DPhe^7, Lys^{10}]-α-MSH(4-10)-NH_2 with bulky aromatic amino acids at position 7 show high antagonist potency and selectivity at specific melanocortin receptors. J Med Chem;38:3454–3461.
21. Shutter J.R., Graham M., Kinsey A.C., Scully S., Luthy R., Stark K.L. (1997) Hypothalamic expression of art, a novel gene related to agouti, is up-regulated in obese and diabetic mutant mice. Genes Dev;11:593–602.
22. Rossi M., Kim M.S., Morgan D.G., Small C.J., Edwards C.M., Sunter D., Abusnana S., Goldstone A.P., Russell S.H., Stanley S.A., Smith D.M., Yagaloff K., Ghatei M.A., Bloom S.R. (1998) A C-terminal fragment of agouti-related protein increases feeding and antagonizes the effect of alpha-melanocyte stimulating hormone in vivo. Endocrinology;139:4428–4431.
23. Hagan M.M., Rushing P.A., Pritchard L.M., Schwartz M.W., Strack A.M., Van Der Ploeg L.H., Woods S.C., Seeley R.J. (2000) Long-term orexigenic effects of AGRP-(83–132) involve mechanisms other than melanocortin receptor blockade. Am J Physiol Regul Integr Comp Physiol;279:R47–52.
24. Graham M., Shutter J.R., Sarmiento U., Sarosi I., Stark K.L. (1997) Overexpression of AGRT leads to obesity in transgenic mice. Nat Genet;17:273–274.
25. Chai B.X., Pogozheva I.D., Lai Y.M., Li J.Y., Neubig R.R., Mosberg H.I., Gantz I. (2005) Receptor-antagonist interactions in the complexes of agouti and agouti-related protein with human melanocortin 1 and 4 receptors. Biochemistry;44:3418–3431.
26. Haskell-Luevano C., Monck E.K. (2001) Agouti-related protein functions as an inverse agonist at a constitutively active brain melanocortin-4 receptor. Regul Pept;99:1–7.
27. Nijenhuis W.A., Oosterom J., Adan R.A. (2001) Agrp(83–132) acts as an inverse agonist on the human-melanocortin-4 receptor. Mol Endocrinol;15:164–171.
28. Yeo G.S., Farooqi I.S., Aminian S., Halsall D.J., Stanhope R.G., O'Rahilly S. (1998) A frameshift mutation in MC4R associated with dominantly inherited human obesity. Nat Genet;20:111–112.
29. Vaisse C., Clement K., Guy-Grand B., Froguel P. (1998) A frameshift mutation in human MC4R is associated with a dominant form of obesity. Nat Genet;20:113–114.
30. Ho G., MacKenzie R.G. (1999) Functional characterization of mutations in melanocortin-4 receptor associated with human obesity. J Biol Chem;274:35816–35822.
31. Ohshiro Y., Sanke T., Ueda K., Shimajiri Y., Nakagawa T., Tsunoda K., Nishi M., Sasaki H., Takasu N., Nanjo K. (1999) Molecular scanning for mutations in the melanocortin-4 receptor gene in obese/diabetic Japanese. Ann Hum Genet;63:483–487.
32. Mergen M., Mergen H., Ozata M., Oner R., Oner C. (2001) A novel melanocortin 4 receptor (MC4R) gene mutation associated with morbid obesity. J Clin Endocrinol Metab;86:3448.
33. Rosmond R., Chagnon M., Bouchard C., Bjorntorp P. (2001) A missense mutation in the human melanocortin-4 receptor gene in relation to abdominal obesity and salivary cortisol. Diabetologia;44:1335–1338.
34. Kobayashi H., Ogawa Y., Shintani M., Ebihara K., Shimodahira M., Iwakura T., Hino M., Ishihara T., Ikekubo K., Kurahachi H., Nakao K. (2002) A novel homozygous missense mutation of melanocortin-4 receptor (MC4R) in a Japanese woman with severe obesity. Diabetes;51:243–246.
35. Lubrano-Berthelier C., Durand E., Dubern B., Shapiro A., Dazin P., Weill J., Ferron C., Froguel P., Vaisse C. (2003) Intracellular retention is a common characteristic of childhood obesity-associated MC4R mutations. Hum Mol Genet;12:145–153.
36. Lubrano-Berthelier C., Le Stunff C., Bougneres P., Vaisse C. (2004) A homozygous null mutation delineates the role of the melanocortin-4 receptor in humans. J Clin Endocrinol Metab;89:2028–2032.
37. Yeo G.S., Lank E.J., Farooqi I.S., Keogh J., Challis B.G., O'Rahilly S. (2003) Mutations in the human melanocortin-4 receptor gene associated with severe familial obesity disrupts receptor function through multiple molecular mechanisms. Hum Mol Genet;12:561–574.
38. Marti A., Corbalan M.S., Forga L., Martinez J.A., Hinney A., Hebebrand J. (2003) A novel nonsense mutation in the melanocortin-4 receptor associated with obesity in a Spanish population. Int J Obes Relat Metab Disord;27:385–388.
39. Farooqi I.S., Yeo G.S., Keogh J.M., Aminian S., Jebb S.A., Butler G., Cheetham T., O'Rahilly S. (2000) Dominant and recessive inheritance of morbid obesity associated with melanocortin 4 receptor deficiency. J Clin Invest;106:271–279.
40. Nijenhuis W.A., Garner K.M., van Rozen R.J., Adan R.A. (2003) Poor cell surface expression of human melanocortin-4 receptor mutations associated with obesity. J Biol Chem;278:22939–22945.
41. Tao Y.X., Segaloff D.L. (2003) Functional characterization of melanocortin-4 receptor mutations associated with childhood obesity. Endocrinology;144:4544–4551.
42. Hinney A., Hohmann S., Geller F., Vogel C., Hess C., Wermter A.K., Brokamp B., Goldschmidt H., Siegfried W., Remschmidt H., Schafer H., Gudermann T., Hebebrand J. (2003) Melanocortin-4 receptor gene: case-control study and transmission disequilibrium test confirm that functionally relevant mutations are compatible with a major gene effect for extreme obesity. J Clin Endocrinol Metab;88:4258–4267.
43. Tarnow P., Schoneberg T., Krude H., Gruters A., Biebermann H. (2003) Mutationally induced disulfide bond formation within the third extracellular loop causes melanocortin 4 receptor inactivation in patients with obesity. J Biol Chem;278:48666–48673.
44. Ma L., Tataranni P.A., Bogardus C., Baier L.J. (2004) Melanocortin 4 receptor gene variation is associated with severe obesity in Pima Indians. Diabetes;53:2696–2699.
45. Valli-Jaakola K., Lipsanen-Nyman M., Oksanen L., Hollenberg A.N., Kontula K., Bjorbaek C., Schalin-Jantti C. (2004) Identification and characterization of melanocortin-4 receptor gene mutations in morbidly obese Finnish children and adults. J Clin Endocrinol Metab;89:940–945.
46. Donohoue P.A., Tao Y.X., Collins M., Yeo G.S., O'Rahilly S., Segaloff D.L. (2003) Deletion of codons 88–92 of the melanocortin-4 receptor gene: a novel deleterious mutation in an obese female. J Clin Endocrinol Metab;88:5841–5845.
47. Larsen L.H., Echwald S.M., Sorensen T.I., Andersen T., Wulff B.S., Pedersen O. (2005) Prevalence of mutations and functional analyses of melanocortin 4 receptor variants identified among 750 men with juvenile-onset obesity. J Clin Endocrinol Metab;90:219–224.
48. Holder J.R., Bauzo R.M., Xiang Z., Haskell-Luevano C. (2002) Structure-activity relationships of the melanocortin tetrapeptide Ac-His-DPhe-Arg-Trp-NH_2 at the mouse melanocortin receptors: Part 2. Modifications at the Phe position. J Med Chem;45:3073–3081.
49. Haskell-Luevano C., Cone R.D., Monck E.K., Wan Y.P. (2001) Structure activity studies of the melanocortin-4 receptor by in vitro mutagenesis: identification of agouti-related protein (AGRP), melanocortin agonist and synthetic peptide antagonist interaction determinants. Biochemistry;40:6164–6179.
50. Chen C.A., Okayama H. (1988) Calcium phosphate-medicated gene transfer: a highly efficient transfections system for stably transforming cells with plasmid DNA. Biotechniques;6:632–638.
51. Chen W., Shields T.S., Stork P.J., Cone R.D. (1995) A colorimetric assay for measuring activation of Gs- and Gq-coupled signaling pathways. Anal Biochem;226:349–354.
52. Schild H.O. (1947) PA_2, a new scale for the measurement of drug antagonism. Br J Pharmacol Chemother;2:189–206.
53. Kopp P., van Sande J., Parma J., Duprez L., Gerber H., Joss E., Jameson J.L., Dumont J.E., Vassart G. (1995) Brief report: Congenital hyperthyroidism caused by a mutation in the thyrotropin-receptor gene. N Engl J Med;332:150–154.

54. Yang Y.K., Thompson D.A., Dickinson C.J., Wilken J., Barsh G.S., Kent S.B., Gantz I. (1999) Characterization of agouti-related protein binding to melanocortin receptors. Mol Endocrinol;13:148–155.
55. Bowen W.P., Jerman J.C. (1995) Nonlinear regression using spreadsheets. Trends Pharmacol Sci;16:413–417.
56. Litherland S.A., Xie X.T., Hutson A.D., Wasserfall C., Whittaker D.S., She J.-X., Hofig A., Dennis M.A., Fuller D.K., Cook R., Schatz D., Moldawer L.L., Clare-Salzler M.J. (1999) Aberrant prostaglandin synthase 2 expression defines an antigen-presenting cell defect for insulin-dependent diabetes mellitus. J Clin Invest;104:515–523.
57. Pogozheva I.D., Chai B.X., Lomize A.L., Fong T.M., Weinberg D.H., Nargund R.P., Mulholland M.W., Gantz I., Mosberg H.I. (2005) Interactions of human melanocortin 4 receptor with small-molecule agonists. Biochemistry;44:11329–11341.
58. Li J., Edwards P.C., Burghammer M., Villa C., Schertler G.F. (2004) Structure of bovine rhodopsin in a trigonal crystal form. J Mol Biol;343:1409–1438.
59. Fowler C.B., Pogozheva I.D., Lomize A.L., LeVine H. 3rd, Mosberg H.I. (2004) Complex of an active mu-opioid receptor with a cyclic peptide agonist modeled from experimental constraints. Biochemistry;43:15796–15810.
60. Riek R.P., Rigoutsos I., Novotny J., Graham R.M. (2001) Non-alpha-helical elements modulate polytopic membrane protein architecture. J Mol Biol;306:349–362.
61. Brooks B.R., Bruccoleri R.E., Olafson B.D., States D.J., Swaminathan S., Karplus M. (1983) CHARMM: a program for macromolecular energy, minimization, and dynamics calculation. J Comput Chem;4:187–217.
62. Ballesteros J.A., Weinstein H. (1995) Integrated methods for the construction of three-dimensional models and computational probing of structure-function relations in G protein coupled receptors. Methods Neurosci;25:366–428.
63. Sawyer T.K., Sanfillippo P.J., Hruby V.J., Engel M.H., Heward C.B., Burnett J.B., Hadley M.E. (1980) 4-Norleucine, 7-D-phenylalanine-α-melanocyte-stimulating hormone: a highly potent α-melanotropin with ultra long biological activity. Proc Natl Acad Sci U S A;77:5754–5758.
64. Srinivasan S., Lubrano-Berthelier C., Govaerts C., Picard F., Santiago P., Conklin B.R., Vaisse C. (2004) Constitutive activity of the melanocortin-4 receptor is maintained by its N-terminal domain and plays a role in energy homeostasis in humans. J Clin Invest;114:1158–1164.
65. Broberger C., Johansen J., Johansson C., Schalling M., Hokfelt T. (1998) The neuropeptide Y/agouti gene-related protein (AGRP) brain circuitry in normal, anorectic, and monosodium glutamate-treated mice. Proc Natl Acad Sci U S A;95:15043–15048.
66. Haskell-Luevano C., Chen P., Li C., Chang K., Smith M.S., Cameron J.L., Cone R.D. (1999) Characterization of the neuroanatomical distribution of agouti related protein (AGRP) immunoreactivity in the rhesus monkey and the rat. Endocrinology;140:1408–1415.
67. Cowley M.A., Smart J.L., Rubinstein M., Cerdan M.G., Diano S., Horvath T.L., Cone R.D., Low M.J. (2001) Leptin activates anorexigenic POMC neurons through a neural network in the arcuate nucleus. Nature;411:480–484.
68. Watson S.J., Barchas J.D., Li C.H. (1977) Beta-lipotropin: localization of cells and axons in rat brain by immunocytochemistry. Proc Natl Acad Sci U S A;74:5155–5158.
69. Haskell-Luevano C., Chen P., Li C., Chang K., Smith M.S., Cameron J.L., Cone R.D. (1999) Characterization of the neuroanatomical distribution of agouti-related protein immunoreactivity in the rhesus monkey and the rat. Endocrinology;140:1408–1415.
70. Jacobowitz D.M., O'Donohue T.L. (1978) Alpha-melanocyte stimulating hormone: immunohistochemical identification and mapping in neurons of rat brain. Proc Natl Acad Sci U S A;75:6300–6304.
71. Khachaturian H., Lewis M.E., Haber S.N., Akil H., Watson S.J. (1984) Proopiomelanocortin peptide immunocytochemistry in rhesus monkey brain. Brain Res Bull;13:785–800.
72. Finley J.C., Lindstrom P., Petrusz P. (1981) Immunocytochemical localization of beta-endorphin-containing neurons in the rat brain. Neuroendocrinology;33:28–42.
73. Thornton J.E., Cheung C.C., Clifton D.K., Steiner R.A. (1997) Regulation of hypothalamic proopiomelanocortin mRNA by leptin in ob/ob mice. Endocrinology;138:5063–5066.
74. Mizuno T.M., Kleopoulos S.P., Bergen H.T., Roberts J.L., Priest C.A., Mobbs C.V. (1998) Hypothalamic pro-opiomelanocortin mRNA is reduced by fasting and corrected in ob/ob and db/db mice, but is stimulated by leptin. Diabetes;47:294–297.
75. Pei G., Samama P., Lohse M., Wang M., Codina J., Lefkowitz R.J. (1994) A constitutively active mutant beta 2-adrenergic receptor is constitutively desensitized and phosphorylated. Proc Natl Acad Sci U S A;91:2699–2702.
76. Jin S., Cornwall M.C., Oprian D.D. (2003) Opsin activation as a cause of congenital night blindness. Nat Neurosci;6:731–735.
77. Kenakin T. (2004) Efficacy as a vector: the relative prevalence and paucity of inverse agonism. Mol Pharmacol;65:2–11.
78. Costa T., Herz A. (1989) Antagonists with negative intrinsic activity at delta opioid receptors coupled to GTP-binding proteins. Proc Natl Acad Sci U S A;86:7321–7325.
79. Okada T., Ernst O.P., Palczewski K., Hofmann K.P. (2001) Activation of rhodopsin: new insights from structural and biochemical studies. Trends Biochem Sci;26:318–324.
80. Meng E.C., Bourne H.R. (2001) Receptor activation: what does the rhodopsin structure tell us? Trends Pharmacol Sci;22:587–593.
81. Gether U., Asmar F., Meinild A.K., Rasmussen S.G. (2002) Structural basis for activation of G-protein-coupled receptors. Pharmacol Toxicol;91:304–312.
82. Patel A.B., Crocker E., Reeves P.J., Getmanova E.V., Eilers M., Khorana H.G., Smith S.O. (2005) Changes in interhelical hydrogen bonding upon rhodopsin activation. J Mol Biol;347:803–812.
83. Fritze O., Filipek S., Kuksa V., Palczewski K., Hofmann K.P., Ernst O.P. (2003) Role of the conserved NPXXY(X)5,6F motif in the rhodopsin ground state and during activation. Proc Natl Acad Sci U S A;100:2290–2295.
84. Li B., Nowak N.M., Kim S.K., Jacobson K.A., Bagheri A., Schmidt C., Wess J. (2005) Random mutagenesis of the m3 muscarinic acetylcholine receptor expressed in yeast: identification of second-site mutations that restore function to a coupling-deficient mutant m3 receptor. J Biol Chem;280:5664–5675.
85. Zhang M., Mizrachi D., Fanelli F., Segaloff D.L. (2005) The formation of a salt bridge between helices 3 and 6 is responsible for the constitutive activity and lack of hormone responsiveness of the naturally occurring L457R mutation of the human lutropin receptor. J Biol Chem;280:26169–26176.
86. Alves I.D., Cowell S.M., Salamon Z., Devanathan S., Tollin G., Hruby V.J. (2004) Different structural states of the proteolipid membrane are produced by ligand binding to the human delta-opioid receptor as shown by plasmon-waveguide resonance spectroscopy. Mol Pharmacol;65:1248–1257.
87. Devanathan S., Yao Z., Salamon Z., Kobilka B., Tollin G. (2004) Plasmon-waveguide resonance studies of ligand binding to the human beta 2-adrenergic receptor. Biochemistry;43:3280–3288.
88. Kobilka B.K. (2002) Agonist-induced conformational changes in the beta2 adrenergic receptor. J Pept Res;60:317–321.
89. Alves I.D., Ciano K.A., Boguslavski V., Varga E., Salamon Z., Yamamura H.I., Hruby V.J., Tollin G. (2004) Selectivity, cooperativity, and reciprocity in the interactions between the delta-opioid receptor, its ligands, and g-proteins. J Biol Chem;279:44673–44682.
90. Han M., Smith S.O., Sakmar T.P. (1998) Constitutive activation of opsin by mutation of methionine 257 on transmembrane helix 6. Biochemistry;37:8253–8261.